DAΦNE TECHNICAL NOTE

INFN - LNF, Accelerator Division

MAGNETIC MEASUREMENTS ON THE LARGE SEXTUPOLES FOR THE DAΦNE MAIN RINGS ACHROMATS

B. Bolli, F. Iungo, F. Losciale, N. Ganlin,
M. Preger, C. Sanelli, F. Sardone

1. Introduction

The series production of the large sextupoles for the DA NE Main Rings achromats, built by ANSALDO, has been delivered to LNF in three batches, the first one (5 magnets) on October 21, the second (6 magnets) on November 5, the third (6 magnets) on December 16, 1996. The characteristics of this kind of multipole have been measured on the prototype and are described in [1]. Here we present the measurements performed with the rotating coil system [2] on all the 18 magnets. The sextupoles are labelled by their serial number, while the label on the prototype is "prototipo". For sake of simplicity, in all the tables presented in this Note, we label the prototype as serial #0. The series production magnets have been measured in two weeks, from 4/12/96 to 19/12/96.

A couple of these sextupoles are placed in each of the 8 achromats of the DA NE Main Rings. The last two are used in the short arcs near the KLOE interaction region, where a large vacuum chamber is foreseen to tag the electrons in coincidence with - interactions [3]. Tables I and II list the integrated gradients (in T/m) required to cancel the chromaticity in both planes, defined as the second derivative of the field times the magnetic length of the sextupoles, in the different configurations of the lattice at the nominal energy of 0.51 GeV. For the names and positions of the sextupoles in the lattice and the name of the different configurations we refer to [4]. The negative sign is used for a horizontally focusing sextupole.

Table I - Integrated gradients for $Q_x = 5.09$, $Q_y = 6.07$

	DD	GD	KD	DF	KF
SXPES101	-1.70	-1.70	-4.42	-4.25	-1.70
SXPES102	16.09	14.88	4.24	18.54	15.76
SXPES103	-3.12	-3,13	-9.00	-4.86	-3.54
SXPES202	-3.12	-3.13	-8.50	-4.25	-4.25
SXPES203	16.09	14.88	17.00	8.50	15.81
SXPEL202	8.50	13.60	17.00	8.50	10.88
SXPEL203	-5.10	-4.51	-5.10	-4.76	-6.80
SXPEL102	-5.10	-4,51	-5.10	-4.93	-6.80
SXPEL103	8.50	13.60	17.00	17.85	10.88

Table I - Integrated gradients for $Q_x = 4.53$, $Q_y = 6.06$

	DD	GD	KD	DF	KF
SXPES101	-1.36	-1.19	1.70	-1.70	-0.85
SXPES102	14.59	11.48	17.42	19.07	7.68
SXPES103	-4.96	-6.94	-4.60	-2.17	-9.99
SXPES202	-4.96	-6.94	-5.87	-11.90	-11.05
SXPES203	14.59	11.48	10.20	5.10	15.30
SXPEL202	12.58	15.47	11.90	13.60	15.47
SXPEL203	-6.46	-5.61	-5.95	-5.95	-5.10
SXPEL102	-6.46	-5.61	-5.95	-5.95	-5.10
SXPEL103	12.58	15.47	11.90	11.90	13.77

Due to the wide spread of the nominal working points, the measurements have been performed at 8 excitation currents in steps of 50 A with the addition of two "historical" points set in the Specifications (50A, 78A, 100A, 150A, 200, 210, 226A and 250A), covering a range of integrated gradients up to 40 T/m. The magnetic length [1] is 154 mm @ 78A and drops down to 151 mm due to saturation in the yoke @ 210A. As shown in Tables I and II, there is a safety margin larger than 2 in the available sextupole strength, allowing to reach positive chromaticity values and to use the ring at higher energy.

Table III - Magnetic center positions and rotations

Serial#	Slit A	Slit B	YA (mm)	YB (mm)	(mrad)
0	12.520	12.450	500.09	499.96	0.21
1	12.420	13.020	500.15	500.12	0.48
2	12.530	12.750	500.34	500.28	-0.03
3	12.330	13.060	500.00	499.97	0.35
4	12.680	12.360	499.99	499.96	-0.50
5	12.340	12.850	500.05	500.00	0.18
6	12.600	12.470	499.95	499.93	-0.17
7	12.195	13.255	500.12	500.09	0.60
8	12.460	12.890	500.14	500.11	-0.02
9	12.450	12.565	500.19	500.16	0.69
10	13.060	12.660	500.05	500.05	-0.26
11	12.920	11.840	500.02	500.01	-1.05
12	12.765	12.540	500.11	500.11	-0.63
13	13.160	12.880	500.12	500.11	0.37
14	12.665	12.760	500.14	500.13	-0.03
15	13.265	12.925	500.07	500.07	0.04
16	12.425	12.435	500.09	500.08	0.48
17	13.350	12.530	500.03	500.05	-0.42

The position of the magnetic centre has also been recorded with respect to the reference optical devices placed on top of the magnets. The mechanical center positions, however, have not yet been measured, and therefore the distance between magnetic and mechanical centres is not yet available. This important part of the magnet characterisation, which takes into account the tilt of the magnet axis (not detectable by the rotating coil system) will be performed by the Alignment Group directly in the DA NE Hall.

Table III shows the positions of the magnetic centers of the sextupoles, referred to the alignment table S1L: the horizontal positions in the second and third columns are the readings of the slits holding the Taylor-Hobson spheres, while the vertical ones (fourth and fifth columns) are the distances between the sphere centers and the position of the magnetic center. The last column gives the rotation of the horizontal magnetic plane with respect to the mechanical one, defined as the horizontal plane of the alignment table. A positive sign of this angle means that the magnet must be rotated counterclockwise by the corresponding angle, looking at it from the hydraulic and electrical connection side, in order to make the horizontal magnetic symmetry plane coincident with the horizontal plane of the ring.

2. Integrated gradient

Table IV gives the integrated gradients measured for each sextupole at the above mentioned excitation currents. Figure 1 is an histogram of the same result at 200.9 A. The distribution is smooth and the standard deviation is 0.2%. Although this figure shows that the uniformity of the series production is satisfactory, it is worth reminding that each magnet has its own independent power supply. Figure 2 shows the average value of the integrated gradient versus the excitation current together with the r.m.s. width of the distributions. The fluctuations of the width are explained by the weak statistical accuracy due to the small number of magnets.

Table IV - Integrated gradients (second derivative x magnetic length, T/m)
at different excitation currents (A)

| Serial#	50.27	78.72	100.50	150.70	200.90	210.25	226.04	251.14
0	8.728	13.662	17.397	25.949	34.086	35.422	-	39.740
1	8.703	13.599	17.312	25.808	33.811	35.094	36.956	39.295
2	8.724	13.632	17.358	25.881	33.924	35.215	37.088	39.442
3	8.713	13.612	17.332	25.847	33.859	35.135	36.982	39.317
4	8.733	13.647	17.381	25.923	34.001	35.295	37.167	39.524
5	8.724	13.524	17.262	25.852	33.931	35.217	37.090	39.447
6	8.705	13.603	17.323	25.832	33.880	35.172	37.060	39.420
7	8.722	13.628	17.354	25.879	33.932	35.222	37.092	39.442
8	8.728	13.634	17.360	25.889	33.922	35.209	37.085	39.448
9	8.737	13.647	17.377	25.918	33.976	35.259	37.123	39.477
10	8.729	13.639	17.366	25.896	33.958	35.257	37.143	39.506
11	8.703	13.600	17.318	25.827	33.827	35.092	36.929	39.260
12	8.718	13.620	17.344	25.863	33.869	35.140	36.989	39.331
13	8.714	13.615	17.336	25.848	33.864	35.146	37.009	39.353
14	8.721	13.623	17.347	25.870	33.894	35.175	37.036	39.387
15	8.702	13.598	17.313	25.813	33.836	35.115	36.973	39.317
16	8.741	13.655	17.386	25.930	33.998	35.290	37.171	39.549
17	8.731	13.639	17.368	25.894	33.917	35.189	37.040	39.380
Aver.	**8.721**	**13.621**	**17.346**	**25.873**	**33.916**	**35.202**	**37.055**	**39.424**
r.m.s	**0.012**	**0.031**	**0.033**	**0.041**	**0.070**	**0.083**	**0.074**	**0.114**
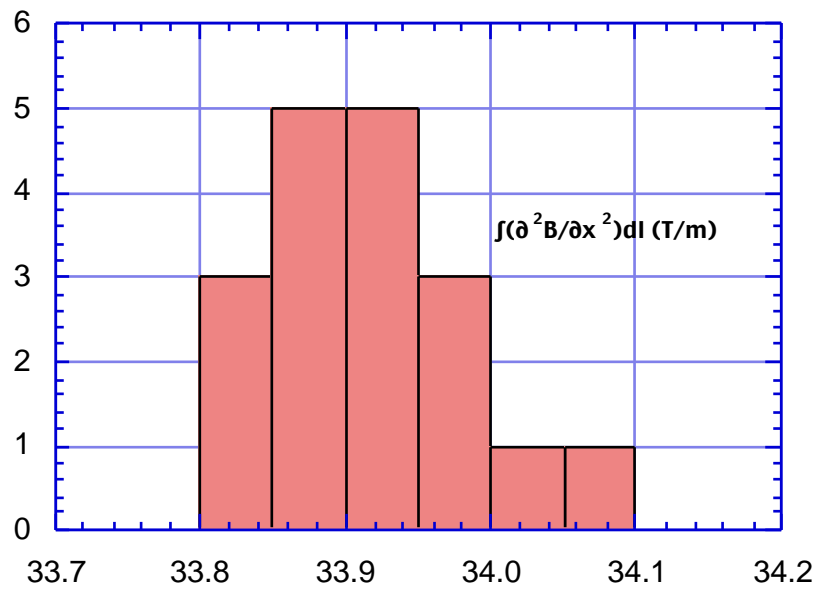
Figure 1. Distribution of integrated gradients among the 18 sextupoles @ 200.9A
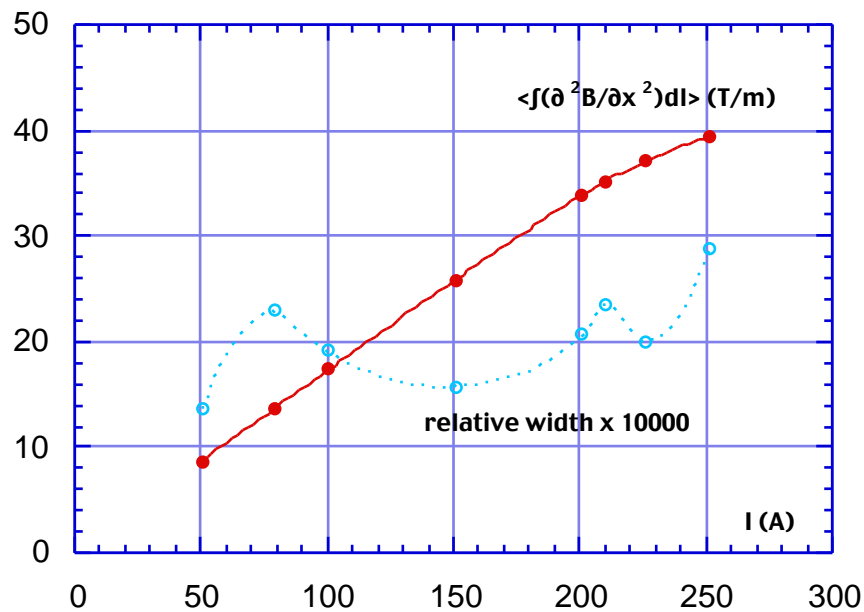(expanded scale)

Figure 2. Average integrated gradient and relative r.m.s width of the distribution
versus current.

2. Average deviation from the ideal field

The average deviation of the field from the ideal sextupole (see [5] for the definition) at the boundary of the good field region is given in Table V for each sextupole. Figure 3 is a typical output of the field deviation on the 30 mm radius circumference limiting the good field region. Figure 4 is an histogram of the $<|\Delta B/B|>$ distribution @ 200.9 A, while Figure 5 shows the same quantity averaged over the 18 magnets versus the excitation current on an expanded scale (error bars are the r.m.s width of the distributions).

The field quality is remarkably constant over the sample of magnets: the deviation from the average is always less than ±7%. The most significant contributions come from the octupole, decapole and 18-pole high order harmonics.

Table V - Average deviation ⊿B/B from the ideal field at 30 mm from the magnet axis (units of 10^{-4}) at different excitation currents (A)

| Serial#	50.27	78.72	100.50	150.70	200.90	210.25	226.04	251.14
0	8.070	8.060	8.090	8.090	8.110	8.270	-	9.160
1	8.311	8.385	8.597	8.460	8.623	8.626	8.462	8.523
2	8.379	8.409	8.157	8.245	8.228	8.175	8.135	8.091
3	8.453	8.714	8.602	8.713	8.911	8.936	9.361	9.487
4	8.420	8.568	8.346	8.387	8.349	8.348	8.305	8.271
5	8.384	8.303	8.351	8.428	8.751	8.549	8.573	8.534
6	8.115	8.180	8.140	8.140	8.177	8.160	8.278	8.357
7	8.654	8.924	8.691	8.746	8.465	8.347	8.378	8.230
8	8.993	8.907	9.000	9.299	9.275	9.487	9.630	9.899
9	9.255	9.009	8.870	9.101	8.864	8.849	8.977	9.365
10	8.578	8.707	8.630	8.929	8.601	8.426	8.428	8.453
11	8.675	8.533	8.469	8.623	8.761	9.062	9.084	8.914
12	10.430	10.160	10.480	9.757	8.982	9.046	8.865	8.883
13	8.346	8.537	8.329	8.228	8.593	8.742	8.899	9.051
14	8.607	8.591	8.342	8.759	8.266	8.312	8.210	8.302
15	9.080	8.746	8.725	8.817	8.692	8.710	8.499	8.472
16	8.487	8.470	8.524	8.645	8.840	8.953	9.558	10.150
17	9.393	9.320	9.559	9.063	9.391	9.558	9.706	9.755
Aver.	**8.702**	**8.696**	**8.661**	**8.691**	**8.660**	**8.698**	**8.785**	**8.883**
r.m.s.	**0.566**	**0.477**	**0.574**	**0.433**	**0.359**	**0.420**	**0.525**	**0.630**
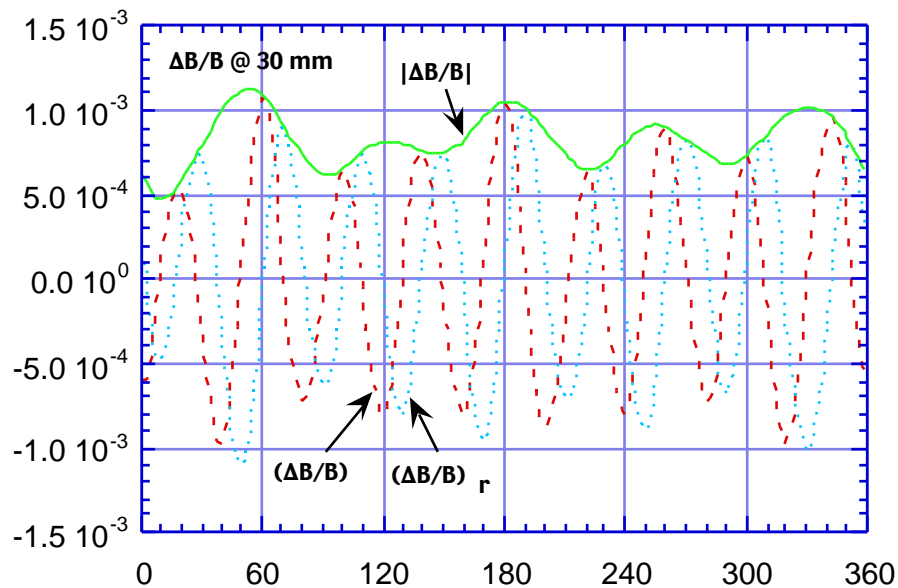
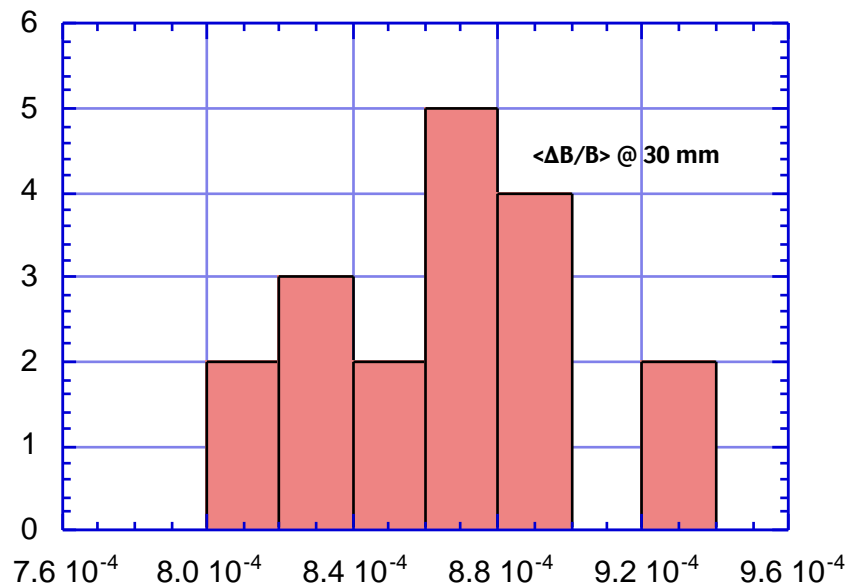Figure 3. Azimuthal, radial and absolute value of relative deviation from ideal sextupole field @ 30 mm from magnet axis (I=200.9A).

Figure 4. Distribution of the average deviation from the ideal sextupole field @ 30 mm
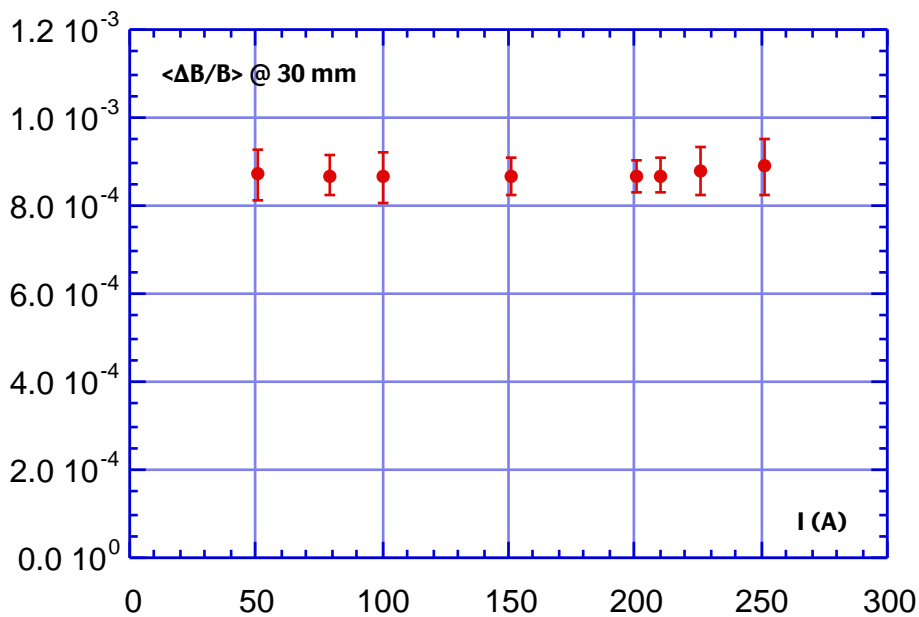from the magnet axis among the 18 sextupoles (I=200.9A, expanded scale)

Figure 5 - Average deviation @ 30 mm averaged over the 18 magnets versus
excitation current. Error bars are the r.m.s. widths of the distributions.

3. Octupole contribution

Table VI lists the octupole component, divided by the main sextupole one for each magnet. Figure 6 shows an histogram of the distribution at 200.9 A. The distribution is rather broad, due to the random origin of the octupole contribution. The dependence of the average values on the excitation current is given in Figure 7 (error bars are the r.m.s. widths of the distributions). Within these widths, the octupole term does not depend on the current and has a large random part. The phase is distributed at random.

Table VI - Octupole/Sextupole @ 30 mm (units of 10^{-4})
at different excitation currents (A)

| Serial#	50.27	78.72	100.50	150.70	200.90	210.25	226.04	251.14
0	0.887	0.201	0.801	0.681	0.466	2.057	-	5.587
1	0.839	0.841	1.929	1.459	2.163	1.759	1.415	2.139
2	2.640	3.326	2.563	2.743	1.508	1.789	1.256	1.029
3	3.555	4.358	4.077	4.322	4.933	5.155	6.072	6.249
4	2.663	3.549	2.421	2.539	1.695	1.713	1.348	1.540
5	2.961	2.844	2.758	2.952	4.599	3.840	3.812	3.419
6	0.662	0.621	0.319	0.408	0.773	0.808	0.767	1.326
7	4.081	4.505	3.095	4.041	3.084	1.820	0.594	1.707
8	5.442	5.245	5.507	6.186	6.029	6.363	6.383	6.686
9	5.922	5.267	4.467	5.095	4.652	4.151	5.145	6.135
10	4.056	4.518	4.187	5.129	3.728	3.220	2.709	2.607
11	3.753	2.839	2.605	2.941	3.796	4.506	4.553	4.148
12	8.105	7.638	8.185	6.917	5.230	5.380	4.828	4.755
13	2.036	2.839	2.193	1.742	3.524	4.086	4.595	5.015
14	3.555	4.050	2.945	4.039	2.160	2.249	2.018	2.198
15	5.303	3.585	4.079	4.428	3.966	4.360	3.327	3.217
16	2.842	2.647	2.716	2.956	3.525	3.413	4.750	5.582
17	5.875	5.822	6.199	4.922	5.614	5.712	5.780	5.596
Aver.	**3.621**	**3.594**	**3.391**	**3.528**	**3.414**	**3.466**	**3.491**	**3.830**
r.m.s.	**1.977**	**1.877**	**1.897**	**1.805**	**1.650**	**1.626**	**1.958**	**1.916**
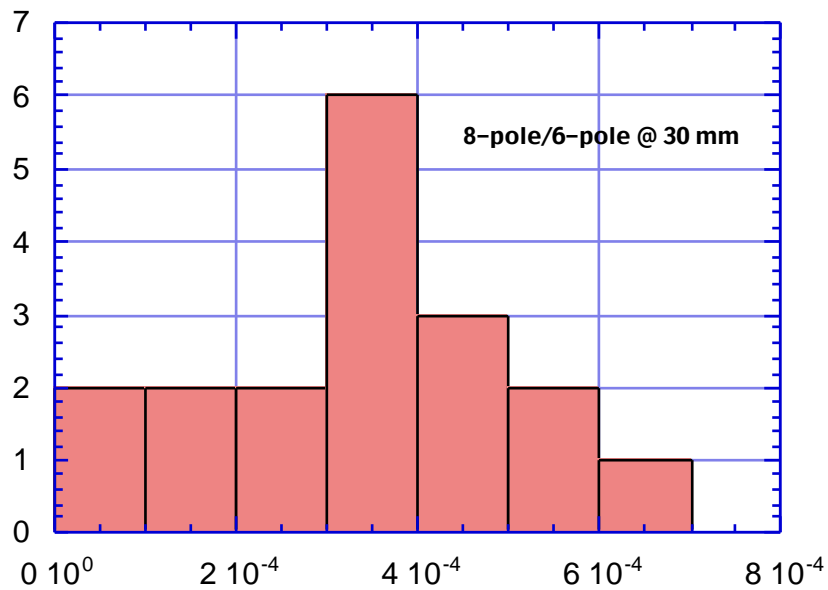
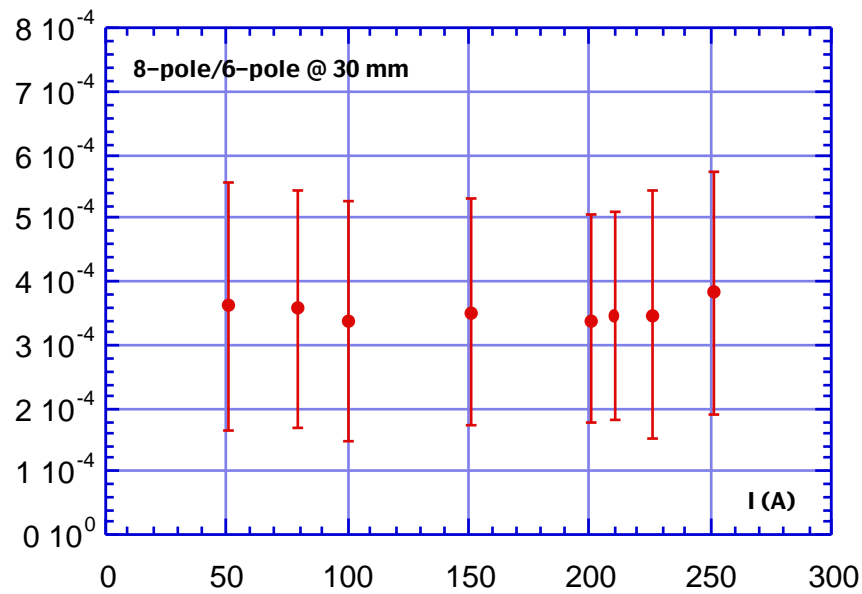Figure 6. Octupole/Sextupole at 30 mm from magnet axis (I=200.9A)..

Figure 7 - Octupole/Sextupole @ 30 mm averaged over the 18 magnets versus excitation current. Error bars are the r.m.s. widths of the distributions.

4. Decapole contribution

Table VII lists the decapole component, divided by the main sextupole one for each magnet, at 30 mm from the magnet axis. Figure 8 is the histogram of the distribution at 200.9 A. As for the octupole contribution, the decapole distribution is broad, due to the random origin of this multipole.
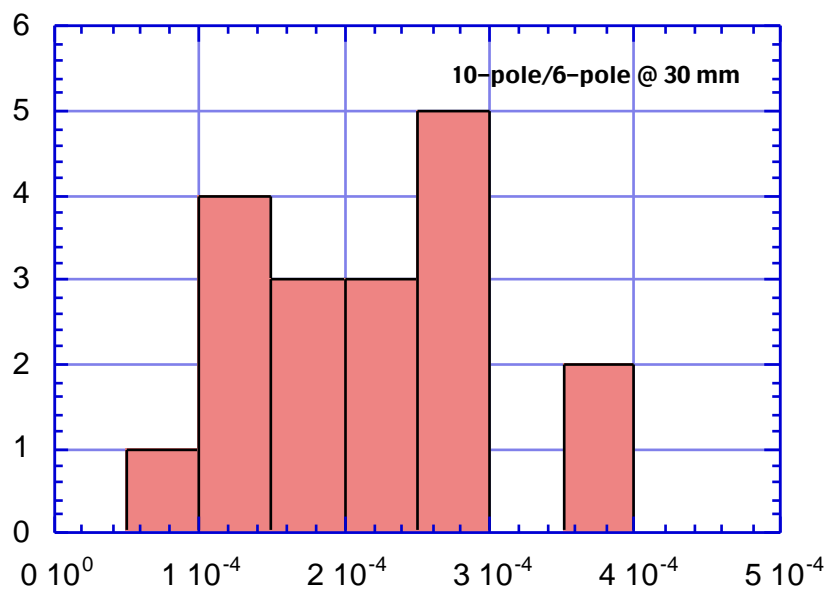

Figure 8. Decapole/Sextupole at 30 mm from magnet axis (I=200.9A).

The dependence of the average values on the excitation current is given in Figure 9 (error bars are the r.m.s. widths of the distributions). Even if the statistical errors are large, it is possible to notice that the decapole contribution increases slightly at large currents. The phase is distributed at random.

Table VII - Decapole/Sextupole @ 30 mm (units of 10^{-4})
at different excitation currents (A)

| Serial#	50.27	78.72	100.50	150.70	200.90	210.25	226.04	251.14
0	0.934	1.354	1.565	1.406	1.555	1.672	-	1.576
1	2.864	3.233	3.707	3.401	3.817	3.813	3.458	3.314
2	2.022	0.848	1.141	0.480	0.999	0.879	1.076	0.917
3	1.386	1.503	1.510	1.655	1.390	1.355	1.429	1.851
4	2.536	2.321	2.186	2.627	2.511	2.833	2.532	2.426
5	0.746	0.879	0.801	0.951	1.023	1.091	1.418	1.976
6	2.030	2.193	2.190	2.399	2.518	2.428	2.768	2.949
7	1.989	2.441	2.776	2.434	2.164	2.684	2.807	2.348
8	0.958	0.514	0.418	0.975	1.468	1.746	2.483	3.088
9	1.469	1.812	2.556	2.366	2.008	2.589	1.929	1.832
10	1.130	0.795	0.796	0.770	1.077	1.200	2.130	2.295
11	2.488	2.941	2.817	3.328	2.956	3.317	3.338	3.054
12	1.831	1.840	1.754	2.061	1.879	1.687	1.768	1.786
13	2.219	2.425	2.071	1.913	1.947	2.117	2.183	2.307
14	2.194	2.076	1.992	2.479	2.086	2.125	1.906	1.875
15	2.442	3.054	2.661	2.419	2.622	2.108	2.222	2.260
16	2.492	2.852	2.826	3.243	3.573	4.135	4.695	5.362
17	2.309	2.056	2.469	2.511	2.796	3.145	3.711	4.079
Aver.	**1.891**	**1.952**	**2.013**	**2.079**	**2.133**	**2.273**	**2.462**	**2.705**
r.m.s.	**0.638**	**0.830**	**0.858**	**0.880**	**0.827**	**0.929**	**0.933**	**1.022**
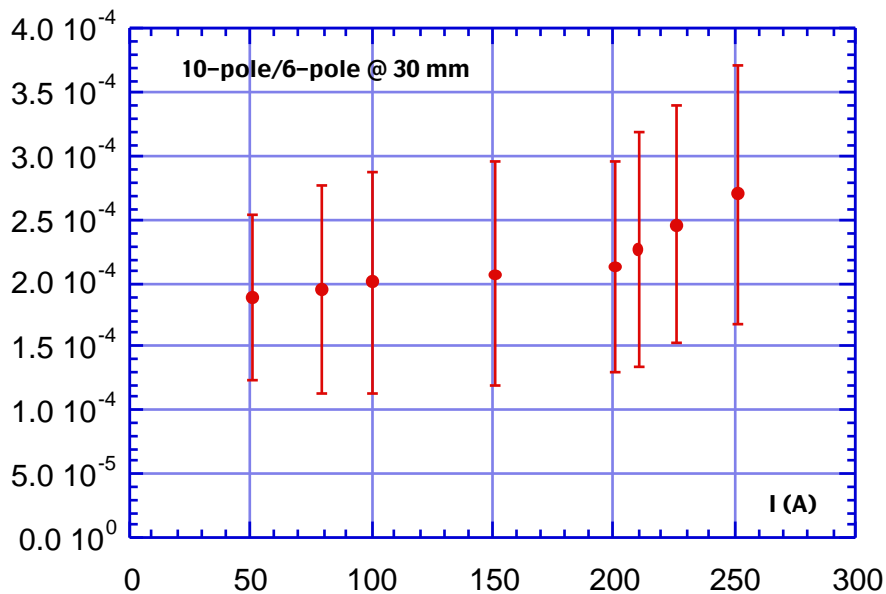
Figure 9 - Decapole/Sextupole @ 30 mm averaged over the 18 magnets versus excitation current. Error bars are the r.m.s. widths of the distributions.

5. 18-pole contribution

The 18-pole, as expected, is the largest contribution to the overall deviation from the ideal field. Table VIII gives its fractional contribution at the boundary of the good field region. Figure 10 is an example of the distribution at 200.9 A.
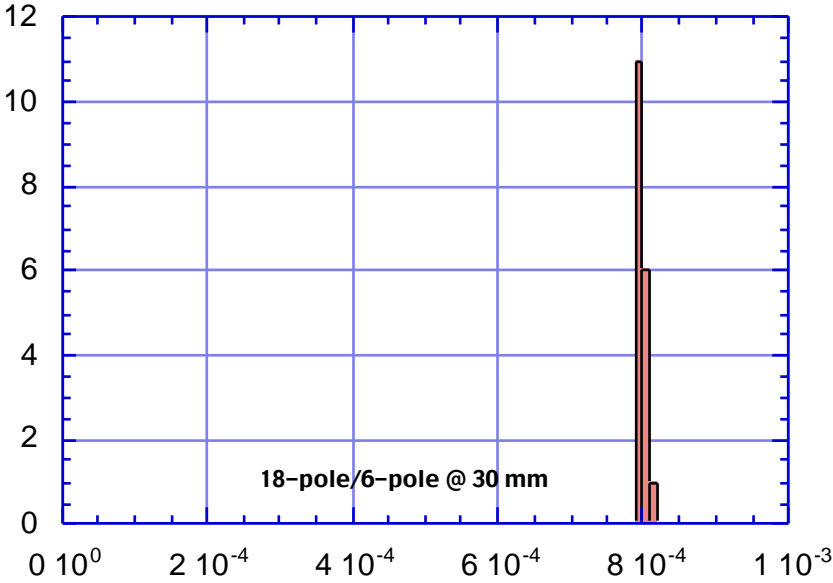
18-pole/6-pole @ 30 mm

Figure 10. 18-pole/Sextupole at 30 mm from magnet axis (I=200.9A).
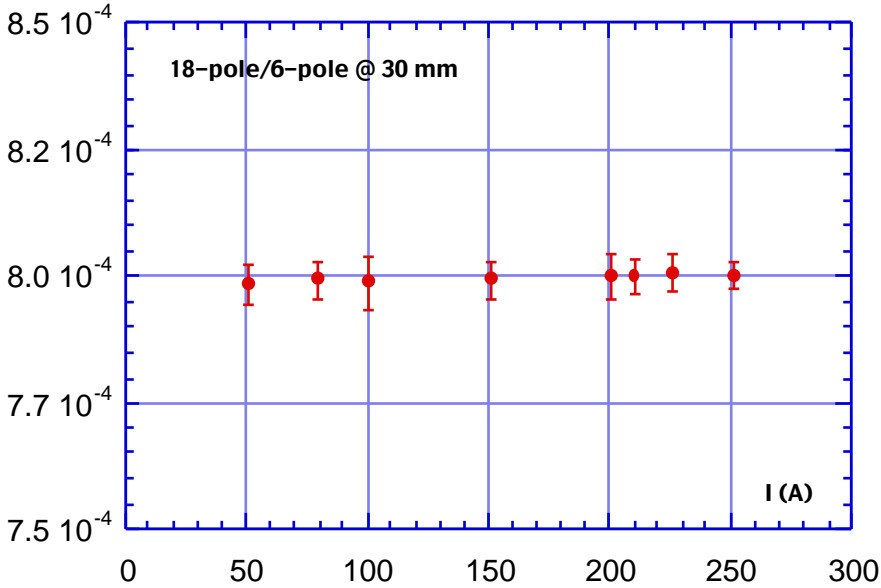
18-pole/6-pole @ 30 mm

I (A)

Figure 11 - 18-pole/Sextupole @ 30 mm averaged over the 18 magnets versus excitation current. Error bars are the r.m.s. widths of the distributions (expanded scale).

Being the 18-pole a systematic multipole with the same symmetry of the main sextupole component, its contribution depends on the pole profile [6], and the distribution has a very small width around the average value. Figure 10 is an histogram of the distribution, while Figure 11 shows, on an expanded scale, its average value over all the magnets and demonstrates that it does not depend on the excitation current. The phase is opposite to the main sextupole component.

Table VIII - 18-pole/Sextupole @ 30 mm (units of 10^{-4})
at different excitation currents (A)

Serial#	50.27	78.72	100.50	150.70	200.90	210.25	226.04	251.14
0	7.935	7.938	7.951	7.959	7.981	7.987	-	7.970
1	8.002	8.008	7.990	7.994	7.972	8.034	7.997	8.002
2	7.977	8.018	7.884	7.968	8.092	8.028	8.013	7.999
3	7.937	7.994	7.953	7.986	8.018	7.967	8.017	8.010
4	7.958	7.949	7.971	7.937	8.024	7.978	8.012	7.976
5	8.050	7.999	8.058	8.079	8.011	8.002	8.017	8.005
6	7.958	8.002	7.982	7.941	7.947	7.948	8.014	8.019
7	7.959	8.056	8.124	7.995	7.982	7.997	8.117	7.967
8	7.987	7.986	7.992	7.979	7.977	7.997	8.016	7.994
9	7.977	7.936	7.975	8.036	7.985	8.041	7.931	7.954
10	7.999	8.018	8.040	8.043	8.107	8.034	8.028	8.047
11	7.988	7.976	7.991	7.972	7.986	7.971	7.976	8.014
12	7.977	8.027	8.001	7.973	7.961	7.996	8.006	8.044
13	8.013	8.050	7.993	7.974	8.028	8.030	8.023	8.008
14	8.054	7.923	7.942	8.026	7.983	8.005	7.963	8.032
15	7.914	8.011	7.927	7.960	7.937	7.919	7.971	7.956
16	8.048	8.003	8.047	8.047	8.042	8.042	8.049	8.029
17	7.984	7.999	7.964	8.006	7.990	8.030	7.983	7.992
Aver.	**7.984**	**7.994**	**7.988**	**7.993**	**8.001**	**8.000**	**8.008**	**8.001**
r.m.s.	**0.039**	**0.037**	**0.054**	**0.039**	**0.045**	**0.035**	**0.040**	**0.028**

6. Conclusions

According to the acceptance criteria already discussed for the small sextupoles for the Accumulator [6] and Main Rings [5], the large sextupoles for the Main Rings achromats are all within the Specifications.

Table IX gives some average values for the systematic and random errors in these sextupoles, to be used in lattice simulations with errors.

Table IX - Systematic and random multipoles
(expressed as fraction of main sextupole field at 30 mm, units of 10^{-4})

Multipole	Systematic	Phase (deg)	Random (rms)	Phase (deg)
8-pole	3.5	random	1.8	random
10-pole	2.2	random	0.9	random
18-pole	8.0	180	-	-

References

[1] B. Bolli, N. Ganlin, F. Iungo, M. Paris, M. Preger, C. Sanelli, F. Sardone, F. Sgamma, M. Troiani "Measurements on Ansaldo sextupole prototype for the DA NE Main Rings (large sextupole)" - DA NE Technical Note MM-12 (26/3/96).

[2] F. Iungo, M. Modena, Q. Qiao, C. Sanelli "DA NE magnetic measurement systems" - DA NE Technical Note MM-1 (2/12/94).

[3] G. Alexander, F. Anulli, D. Babusci, R. Baldini-Ferroli, M. Bassetti, S. Bellucci, I. Cohen, A. Courau, G. Giordano, G. Matone, A. Moalem, M.A. Moinester, G. Pancheri, M. Preger, L. Razdolkaja, P. Sergio, P. Tini-Brunozzi, A. Zallo "Two Photon Physics capabilities of KLOE at DA NE" - LNF-93/030 (P) 21/6/1993

[4] M.E. Biagini, C. Biscari, S. Guiducci "DA NE Main Rings lattice update" - DA NE Technicale Note L-22 (18/3/96)

[5] B. Bolli, F. Iungo, F. Losciale, N. Ganlin, M. Preger, C. Sanelli, F. Sardone "Field quality of the small quadrupoles for the DA NE Main Rings" - DA NE Technical Note MM-10 (22/2/96).

[6] B. Bolli, F. Iungo, M. Modena, M. Paris, M. Preger, C. Sanelli, F. Sardone. F. Sgamma, M. Troiani "The DA NE Accumulator Sextupoles" - DA NE Technical Note MM-6 (10/5/95).